

**This is the accepted manuscript version of the contribution published as:**

Jin, B., Nijenhuis, I., Rolle, M. (2018):

Simulation of dual carbon–bromine stable isotope fractionation during 1,2-dibromoethane degradation

*Isot. Environ. Health Stud.* **54** (4), 418 – 434

**The publisher's version is available at:**

<http://dx.doi.org/10.1080/10256016.2018.1468759>

1 **Simulation of Dual Carbon–Bromine Stable Isotope Fractionation during 1,2-**  
2 **Dibromoethane Degradation**

3  
4 Biao Jin<sup>a,b\*</sup>, Ivonne Nijenhuis<sup>c</sup>, Massimo Rolle<sup>a</sup>

5  
6  
7  
8  
9  
10  
11  
12 <sup>a</sup>Department of Environmental Engineering, Technical University of Denmark, Miljøvej Building  
13 113, DK-2800 Kgs. Lyngby, Denmark

14 <sup>b</sup>State Key Laboratory of Organic Geochemistry, Guangzhou Institute of Geochemistry, Chinese  
15 Academy of Sciences, Kehua Street 511, 510640 Guangzhou, China

16 <sup>c</sup>Department of Isotope Biogeochemistry, Helmholtz-Centre for Environmental Research - UFZ,  
17 Permoserstrasse 15, 04318 Leipzig, Germany

18  
19  
20  
21 \* Corresponding author phone: +45 45251566; e-mail: [bjin@env.dtu.dk](mailto:bjin@env.dtu.dk)

24 **Abstract**

25 We performed a model-based investigation to simultaneously predict the evolution of concentration,  
26 as well as stable carbon and bromine isotope fractionation during 1,2-dibromoethane (EDB,  
27 ethylene dibromide) transformation in a closed system. The modelling approach considers bond-  
28 cleavage mechanisms during different reactions and allows evaluating dual carbon-bromine isotopic  
29 signals for chemical and biotic reactions, including aerobic and anaerobic biological transformation,  
30 dibromoelimination by Zn(0) and alkaline hydrolysis. The proposed model allowed us to accurately  
31 simulate the evolution of concentrations and isotope data observed in a previous laboratory study  
32 and to successfully identify different reaction pathways. Furthermore, we illustrated the model  
33 capabilities in degradation scenarios involving complex reaction systems. Specifically, we  
34 examined (i) the case of sequential multistep transformation of EDB and the isotopic evolution of  
35 the parent compound, the intermediate and the reaction product, and (ii) the case of parallel  
36 competing abiotic pathways of EDB transformation in alkaline solution.

37

38 **Keywords:** degradation; organic contaminants; isotope modelling; compound-specific isotope  
39 analysis; stable carbon and bromine isotopes

40

41

42

## 43 **1. Introduction**

44 In the last few decades, 1,2-dibromoethane (EDB, ethylene dibromide) has been frequently detected  
45 in drinking water and natural aquatic systems, due to its extensive application as an agricultural  
46 fumigant as well as a lead scavenger in gasoline [1,2]. EDB is a widespread pollutant and several  
47 studies have investigated its degradation under different environmental conditions [3–5]. However,  
48 the environmental fate of EDB is difficult to understand and to quantitatively assess since this  
49 chemical can undergo different transformation processes and its concentration distribution in  
50 aquatic systems also depends on physical processes such as mass-transfer, dilution and sorption [6–  
51 8]. Therefore, the application of compound specific isotope analysis (CSIA) is beneficial to  
52 investigate the environmental fate of EDB. CSIA techniques have been developed and applied to a  
53 wide variety of organic pollutants [9–12], for which the determination of the change of stable  
54 isotope signals could be used to identify and quantify specific transformation processes. Carbon is  
55 the most common element for CSIA applications in contaminant hydrology; however, recent  
56 developments on analytical techniques for chlorine and bromine CSIA allowed increasing  
57 applications of dual-element isotope analysis for organohalides [13–18]. Thus, different reaction  
58 pathways of halogenated organic pollutants could be characterized and understood using dual-  
59 element CSIA [19–23]. In a very recent laboratory study, Kuntze et al. [24] applied dual carbon-  
60 bromine CSIA to investigate different reaction mechanisms during EDB degradation.

61 In this work we propose an isotope modelling approach for dual carbon-bromine isotope  
62 fractionation based on the reaction mechanisms and the experimental data from the study of Kuntze  
63 et al. [24]. Isotope models are valuable tools to provide quantitative interpretation of isotopic data  
64 obtained during different transformation processes as well as in complex environmental systems  
65 where both physical and transformation processes influence the observed isotopic signals [25–27].  
66 So far, isotope models have been developed and applied for multi-element isotopic prediction of

67 various organic contaminants, including chlorinated hydrocarbons [28–31], BTEX compounds  
68 [32,33] and organic pesticides [34,35]. However, such a modelling framework is still lacking for  
69 brominated organic compounds. This modelling case study illustrates an integrated carbon-bromine  
70 isotope modelling approach to simultaneously predict the evolution of concentration, as well as  
71 carbon and bromine isotopic signals. Our work focuses on chemical and biotic transformations of  
72 EDB with the specific goals to: (i) describe a mechanism-based integrated modelling approach to  
73 simulate carbon and bromine isotope fractionation; (ii) validate the model with the isotopic data  
74 observed during EDB degradation reactions; (iii) illustrate the capabilities of the model based on  
75 scenarios of complex EDB degradation pathways, including multistep reactions and parallel  
76 degradation pathways, and considering the evolution of dual C and Br isotope signals not only of  
77 EDB but also of its degradation intermediates and products.

78

## 79 **2. Modelling approach**

### 80 ***2.1. Degradation pathways and reaction mechanisms***

81 We focus on EDB degradation through two important degradation pathways, dibromoelimination  
82 and nucleophilic substitution ( $S_N2$ ). The two degradation pathways can occur both chemically and  
83 biotically. Dibromoelimination occurs during reduction of EDB with Zn(0) in aqueous solution, as  
84 well as during biotic transformation by *Sulfurospirillum multivorans*. A stepwise nucleophilic  
85 substitution may take place in aqueous alkaline solution and also occurs during biotic  
86 transformation by *Ancylobacter aquaticus* [24]. The two pathways involve different bond-cleavage  
87 mechanisms. Dibromoelimination is assumed to result in simultaneous cleavage of two C-Br bonds,  
88 while  $S_N2$  reaction follows a stepwise cleavage of one C-Br bond [5,24].

89

90 **2.2. Pathway-specific reaction rates and isotope fractionation**

91 In order to simulate carbon and bromine isotopic evolution of EDB via different reactions, we track  
92 dual element isotopologues. The relative abundances of such isotopologues can be computed  
93 considering the occurrence of both stable carbon and bromine isotopes:

94 where  $A$  is the relative abundance of the  $j^{\text{th}}$  EDB isotopologue containing  $a$   $^{13}\text{C}$  out of a total of two  
95 carbon atoms and  $b$   $^{81}\text{Br}$  out of a total of two bromine atoms.  $X$  and  $Y$  are the abundance of heavy  
96 carbon and bromine isotopes, respectively. (1)

97 Position specific fractionation factors for the  $j^{\text{th}}$  EDB isotopologue can be calculated according to  
98 the corresponding apparent kinetic isotope effect (AKIE) derived from the observed bulk  
99 enrichment factors:

100 where  $\alpha_{rp}$  is the fractionating factor at reactive position,  $\varepsilon$  is bulk enrichment factor, and  $z$  is the  
101 number of carbon or bromine atoms at reactive positions. In this work we calculated  $\alpha_{rp}$  based on  
102 the AKIE values reported in Kuntze et al. (2016); however,  $\alpha_{rp}$  could be also derived by fitting the  
103 proposed model to the raw isotope data. (2)  
(3)

104 We track the concentration change of each isotopologue considering a specific kinetic rate law. To  
105 illustrate the approach, a first-order kinetic formulation is considered in the following equations;  
106 however, as discussed for the application examples in Section 3, any degradation rate can be  
107 implemented, including Michaelis-Menten kinetics. Since different reaction mechanisms of EDB  
108 involve carbon and bromine atoms located at different isotopically-sensitive positions, the reaction  
109 rates have to take into account all the fractionating atoms. Concerning the dibromoelimination  
110 reaction, the two C-Br bonds are cleaved simultaneously, and thus the reaction rate for a specific  
111 carbon-bromine isotopologue is given as:

112 where  $r_j$  is the reaction rate for the  $j^{\text{th}}$  isotopologue,  $k$  is the first-order reaction rate constant,  $C_j$  is  
113 the concentration of the  $j^{\text{th}}$  isotopologue,  $\alpha_{rp}$  is the fractionation factor as defined in Eqs. (2) and (3).

114 Considering  $S_N2$  reaction of EDB, such reaction pathway involves the cleavage of one single C-Br  
115 bond. In this case the reaction rate of EDB depends on the isotopic composition of the C-Br bond  
116 that is cleaved, and thus the reaction rate of the individual isotopologues is defined in a bond-  
117 specific manner as previously proposed for the carbon-chlorine isotope modelling of chlorinated  
118 ethenes [30]. Due to the fact that the two C-Br bonds of EDB are chemically equivalent for  $S_N2$   
119 reaction, the approach is based on isotopologues without the need of specifying individual  
120 isotopomers. Thus, the reaction rate,  $r_j$ , for a given  $j^{\text{th}}$  EDB isotopologue is expressed as the sum of  
121 the following bond-specific reaction rates:

(4)

(5)

(6)

(7)

(8)

(9)

122 where  $k$  is the first-order rate constant,  $C_j$  is the concentration of the  $j^{\text{th}}$  isotopologue, and  $n_{rp}$   
123 represents the total number of reactive carbon or bromine atoms within the isotopologue,  $i$  indicates  
124 the C-Br bond cleaved during the reaction and  $N$  is the total number of C-Br bonds that can be  
125 cleaved for the  $j^{\text{th}}$  EDB isotopologue. Note that an overall rate for all isotopologues can be  
126 computed from the rate of each isotopologue as , where  $m$  is the total number of isotopologues. The  
127 concentration change of the  $j^{\text{th}}$  isotopologue of EDB is described as:

(10)

128 The total concentration of EDB can be obtained by summing the concentrations of each  
129 isotopologue:

(11)

130

131 where  $C_{tot}$  is the total concentration of EDB,  $C_j$  is the concentration of the  $j^{\text{th}}$  isotopologue and  $m$  is  
132 the total number of EDB isotopologues.

133 The concentration of each isotopologue is used to calculate stable carbon and bromine isotope ratios  
134 by considering the total number of heavy and light isotopes [14] and are expressed as:

$$(12)$$

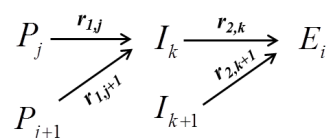
$$(13)$$

135 where  $R_C$  and  $R_{Br}$  are the carbon and bromine isotope ratios of EDB,  $C_j$  is the concentration of the  $j^{\text{th}}$   
136 isotopologue,  $m$  is the total number of EDB isotopologues as defined in Eq (11),  $a$  and  $b$  are the  
137 number of heavy carbon and heavy bromine isotopes, as defined in Eq (1).

### 138 **2.3. Complex Reaction Pathways**

139 In the previous section we illustrated the modelling for single step reactions. However, the model  
140 can be applied also when degradation occurs through more complex reaction pathways involving  
141 sequential and parallel reactions. In this cases, if one aims at describing the formation and  
142 consumption of intermediates and products and the evolution of their dual-element isotopic  
143 composition, it is necessary to take into account that a given intermediate (or product) can be  
144 formed by two distinct isotopologues of the parent compound (or intermediate).

145 Sequential multistep reactions. We consider EDB degradation through sequential multistep  
146 reactions, specifically, through a reaction pathway involving two  $S_N2$  type reactions. As parent  
147 compound ( $P$ ) the two different EDB isotopologues considered are: the  $j^{\text{th}}$  isotopologue and the  
148  $(j+1)^{\text{th}}$  isotopologue. The latter contains one more  $^{81}\text{Br}$  isotope in the molecule compared to the  $j^{\text{th}}$   
149 isotopologue. The parent compound ( $P$ ) is sequentially degraded into the  $k^{\text{th}}$  and  $(k+1)^{\text{th}}$   
150 isotopologues of the intermediate ( $I$ ), and finally into the  $i^{\text{th}}$  isotopologue of the end product ( $E$ ),  
151 which is completely debrominated. The two-step reaction can be illustrated as:



(14)

152

153

154 Note that the different letters used as subscripts indicate that the different compounds may have a  
 155 different number of isotopologues.

156 The concentration of the isotopologues of the parent compound ( $P$ ), the intermediate ( $I$ ) and the end  
 157 product ( $E$ ) are described:

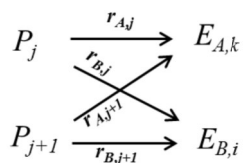
(15)

(16)

(17)

158 where  $r_{1,j}$ ,  $r_{1,j+1}$ ,  $r_{2,k}$  and  $r_{2,k+1}$  are the isotopologue-specific reaction rates for the parent compound and  
 159 for the intermediate, respectively. The kinetic formulation for such reaction rates  $r_{1,j}$  and  $r_{1,j+1}$   
 160 (parent compound), as well as  $r_{2,k}$  and  $r_{2,k+1}$  (intermediate) are based on Eqs. 5-9. The carbon and  
 161 bromine isotope ratios for the parent compound, intermediate and end product can be calculated  
 162 according to Eqs. 12-13.

163 Parallel reactions. Competition between different reaction pathways of EDB degradation has been  
 164 observed in several experimental studies [5,24]. We consider the case of EDB transformation  
 165 through two competing reaction pathways that yield two different products:



(18)

166

167 The concentration of the  $j^{\text{th}}$  isotopologues of the parent compound ( $P_j$ ) and the  $k^{\text{th}}$  and  $i^{\text{th}}$  of the two  
 168 end products ( $E_{A,k}$  and  $E_{B,i}$ ) are given as:

(19)

(20)

(21)

169 where  $r_{A_j}$ ,  $r_{A_{j+1}}$ ,  $r_{B_j}$  and  $r_{B_{j+1}}$  are the reaction rates for the individual reaction pathway of the  $j^{\text{th}}$  and  
170  $(j+1)^{\text{th}}$  isotopologue of the parent compound ( $P$ ).

#### 171 **2.4. Model implementation**

172 The governing equations describing the simultaneous evolution of the concentrations, as well as the  
173 carbon and bromine isotope ratios are implemented in MATLAB<sup>®</sup>. The system of ordinary  
174 differential equations is solved numerically using the function *ode15s*. The experimental data and  
175 the key isotope fractionation parameters are taken from the experimental work of Kuntze et al.  
176 (2016); the latter are summarized in Table 1. The simulation was run for a time covering the  
177 duration of the experiments (i.e., 4 hours for the two cases of dibromoelimination by both Zn(0) and  
178 *S. multivorans*, 350 hours for abiotic degradation in alkaline solution and 8 hours in the case of  
179 biotic degradation by *A. aquaticus*). The EDB concentration data were used to determine the kinetic  
180 parameters of the degradation rates. First-order and Michaelis-Menten kinetics were considered for  
181 the abiotic and biotic reaction pathways, respectively. A fitting procedure, minimizing the sum of  
182 normalized squared errors based on the function *lsqnonlin*, was used to obtain the values of the  
183 kinetic parameters. As illustrated above, the proposed approach tracks the dual-element EDB  
184 isotopologues. Nine EDB isotopologues were considered in the simulations by taking into account  
185 all possible combinations of carbon and bromine isotopes. The abundances of these isotopologues  
186 were determined based on Eq. 1.

187 **[insert Table 1 here]**

188

### 189 **3. Results and discussion**

### 190 3.1. Chemical and biotic dibromoelimination reactions

191 The dual carbon and bromine isotope approach has been used to investigate EDB degradation by  
192 dibromoelimination reactions [24]. To reproduce the experimental data observed during  
193 dibromoelimination reactions, we simulated carbon and bromine isotopic evolution according to the  
194 hypothesized two-electron transfer dibromoelimination mechanism. The simulation results (solid  
195 lines in Fig. 1) are shown together with the reported experimental data (symbols in Fig. 1). A first-  
196 order kinetic ( $k=0.9 \text{ h}^{-1}$ ) is used to describe the concentration variation of EDB during  
197 dibromoelimination by Zn(0) (Fig. 1a), where the concentration decreases down to 4.3% of the  
198 initial concentration value. The model also accurately predicts the carbon and bromine isotope  
199 fractionation (Fig. 1b), which are simulated based on the experimentally evaluated *AKIE* values  
200 ( $AKIE_C=1.0223$ ,  $AKIE_{Br}=1.0042$ ) [24]. The results show different extents of carbon and bromine  
201 fractionation, with  $\delta^{13}\text{C}$  values changing from -26.3‰ to -3.8‰ and  $\delta^{81}\text{Br}$  varying from 0.5‰ to  
202 5.4‰. For biotic dibromoelimination, a Michaelis-Menten kinetics, with maximum degradation rate  
203  $k_{max}=0.2289 \text{ mmol}\cdot\text{L}^{-1}\cdot\text{h}^{-1}$  and half-saturation constant  $K_s=0.0166 \text{ mmol}\cdot\text{L}^{-1}$ , is used in our model to  
204 reproduce the observed concentration data during biotic dibromoelimination by *S. multivorans* (Fig.  
205 1c). The carbon and bromine *AKIE* values of 1.0107 and 1.0046 are used in the model to describe  
206 carbon and bromine isotope effects. The fractionation was introduced in the maximum degradation  
207 rate and led to an increase of 12.7‰ for  $^{13}\text{C}$  and of 6.2‰ for  $^{81}\text{Br}$  isotopes during degradation of  
208 about 95% of the initial EDB concentration.

209 **[insert Figure 1 here]**

210 Linear dual carbon-bromine isotopic trends with different slopes are obtained for chemical (slope of  
211 5.3) and biotic (slope of 2.4) dibromoelimination reactions and the model accurately captures the  
212 two different dual-isotope trends. The excellent agreement between experimental and modelling

213 results demonstrates the capability of the proposed mechanistic model to simultaneously capture the  
214 evolution of both concentration and carbon-bromine stable isotopes.

### 215 **3.2. Chemical and biotic nucleophilic substitution ( $S_N2$ ) reactions**

216 Nucleophilic substitution ( $S_N2$ ) reaction is another important degradation mechanism for EDB. A  
217 stepwise scenario is followed by both biotic and chemical  $S_N2$  reactions, where the cleavage of one  
218 carbon-bromine bond of EDB is hypothesized as the isotopically sensitive step. We provide a  
219 model-based interpretation of the experimental data provided in the study of Kuntze et al. [24], who  
220 observed carbon and bromine isotope fractionation of EDB during chemical degradation in aqueous  
221 alkaline solution as well as during biotic  $S_N2$  reaction by *Ancylobacter aquaticus*.

222 **[insert Figure 2 here]**

223 We use a first-order kinetics ( $k=0.0125\text{ h}^{-1}$ ) to describe the concentration change during the  
224 chemical  $S_N2$  reaction (solid line in Fig. 2a). The corresponding carbon isotope ratio varies from  
225  $-11.6\text{‰}$  to  $93.8\text{‰}$ , and the bromine isotope fractionation occurs in a range between  $0.4\text{‰}$  and  
226  $4.3\text{‰}$ . The biotic  $S_N2$  reaction of EDB is described by a Michaelis-Menten kinetics with maximum  
227 degradation rate ( $k_{max}=0.4329\text{ mmol}\cdot\text{L}^{-1}\cdot\text{h}^{-1}$ ) and half-saturation constant ( $K_s=0.0288\text{ mmol}\cdot\text{L}^{-1}$ )  
228 evaluated based on the observed concentration data (Fig. 2c). The simulation of carbon and bromine  
229 isotope signals is based on the reported  $AKIE$  values ( $AKIE_C=1.062$  and  $AKIE_{Br}=1.002$  for the  
230 chemical  $S_N2$  reaction;  $AKIE_C=1.014$  and  $AKIE_{Br}=1.0012$  for the biotic  $S_N2$  reaction). The  
231 simulations of the biotic and chemical  $S_N2$  transformations of EDB were able to capture the  
232 different fractionation of the two reaction pathways observed in the experiments. Specifically, the  
233 biotic transformation resulted in a smaller extent of both carbon and bromine isotope fractionation  
234 ( $17.9\text{‰}$  for  $\delta^{13}\text{C}$  and  $1.8\text{‰}$  for  $\delta^{81}\text{Br}$ ) whereas the chemical  $S_N2$  reaction resulted in stronger  
235 fractionation ( $105.4\text{‰}$  for  $\delta^{13}\text{C}$  and  $3.9\text{‰}$  for  $\delta^{81}\text{Br}$ ).

236

237 Fig. 3 summarizes the dual element isotope plots for the four cases of chemical and biotic EDB  
238 degradation through dibromoelimination and S<sub>N</sub>2 type nucleophilic substitution. The four different  
239 reactions are adequately characterized in the dual carbon-bromine isotope plot. In all the cases the  
240 simulation outcomes closely reproduce the experimental results. Note that these outcomes are no  
241 linear fits of the experimental data, but represent mechanistic descriptions of EDB degradation  
242 through different reaction pathways according to the approach outlined in Section 2. For all  
243 considered cases of EDB degradation the normalized root mean squared error was calculated as a  
244 quantitative measure of the goodness-of-fit. Such metric was computed for both carbon and  
245 bromine isotope data and yielded values in a range of 0.036-0.158 for carbon and 0.068-0.16 for  
246 bromine. The successful comparison of the simulation results with the experimental data highlights  
247 the capability of the proposed approach to quantitatively describe different mechanisms of EDB  
248 degradation.

249 **[insert Figure 3 here]**

### 250 ***3.3. Scenario modelling***

251 Based on the validated model presented above, we also investigated scenarios involving complex  
252 EDB reaction pathways, such as sequential multistep reactions (Scenario 1 in Fig. 4) and parallel  
253 reactions (Scenario 2 in Fig. 4). In the examples illustrated in the previous section and in most  
254 experimental studies, the CSIA approach has been mainly focusing on the parent compound.  
255 However, stable isotope analysis of reaction products can also be very informative about the  
256 underlying reaction steps characterizing different reaction mechanisms [22,31]. To explore the  
257 potential of carbon and bromine CSIA of EDB degradation products, we simulate the evolution of  
258 the concentration and the isotopic signals of the parent compound, the intermediates and the end

259 products for the two proposed reaction scenarios illustrated in Fig. 4: 1) multistep  $S_N2$  nucleophilic  
260 substitution and 2) simultaneous occurrence of the  $S_N2$  reaction and dehydrobromination.

261 **[insert Figure 4 here]**

262 The  $S_N2$  reaction involves the stepwise cleavage of two C-Br bonds, kinetic isotope effects for C-Br  
263 cleavage ( $KIE_C=1.042$ ;  $KIE_{Br}=1.002$ ) were calculated in the previous experimental study based on  
264 the Streitwieser limit [24]. Since isotope fractionation of the intermediate has not been  
265 experimentally determined (yet), the theoretical  $KIEs$  values are used as model input parameters to  
266 differentiate the reaction rates of the different carbon-bromine isotopologues of both parent and  
267 intermediate compounds. The simulation results for sequential multistep EDB degradation  
268 (Scenario 1) are shown in Fig. 5. The degradation of the parent compound EDB (blue solid line in  
269 Fig. 5a) results in the formation of the intermediate, bromoethylene glycol (red dotted line,  $k=0.5 \text{ h}^{-1}$ )  
270 <sup>1</sup>), which is further transformed to ethylene glycol (green dash-dotted line,  $k=2.5 \text{ h}^{-1}$ ) that  
271 accumulates as the end product. The temporal carbon and bromine isotope trends are reported in  
272 Fig. 5b and 5c and show a linear increase of  $\delta^{13}\text{C}$  and  $\delta^{81}\text{Br}$  values for EDB. However, the  
273 increasing trends of carbon and bromine isotope ratios become nonlinear for the intermediate,  
274 bromoethylene glycol. This is due to the fact that bromoethylene glycol (red dotted line) further  
275 degrades and preferentially transfers  $^{12}\text{C}$  isotopes to the end product and meanwhile preferentially  
276 releases  $^{79}\text{Br}$  during its transformation. As a result, the  $\delta^{13}\text{C}$  values of the end product, ethylene  
277 glycol (green dash-dotted line), continuously increase and approach the original carbon isotope  
278 signature of EDB. In the dual carbon-bromine isotope plot (Fig. 5d) EDB and bromoethylene glycol  
279 have different trends. EDB shows a linear increase with a slope of 20.2, whereas a nonlinear curve,  
280 with a slope varying from 11 to 21.5, describes the trend of bromoethylene glycol. This nonlinear  
281 behaviour is due to the simultaneous formation and consumption of bromoethylene glycol, which  
282 occur at different rates and involve different extents of carbon and bromine isotope fractionation

283 during the course of the degradation reaction. For multistep reactions with formation and further  
284 degradation of intermediates, a mechanistic modelling approach is helpful since it allows the  
285 simultaneous interpretation of isotope fractionation for both precursors and reaction products.

286 **[insert Figure 5 here]**

287 In Scenario 2, degradation of EDB in alkaline solution is considered. In this scenario two competing  
288 reaction pathways, i.e., nucleophilic substitution ( $S_N2$ ) and dehydrobromination, occur  
289 simultaneously. Concerning dehydrobromination, this reaction pathway involves the simultaneous  
290 cleavage of a carbon-bromine bond and a carbon-hydrogen bond. The theoretical carbon and  
291 bromine isotopic effects during cleavage of C-H ( $KIE_C=1.021$ ) and C-Br ( $KIE_C=1.042$ ;  
292  $KIE_{Br}=1.002$ ) bonds [24,36] are considered to calculate the fractionation factors at reactive positions  
293 used in the isotopologue-specific rate expression (Eq. 4). We applied the model to simulate  
294 concentrations and isotope ratios for such a parallel reaction system. We assume that the two  
295 reactions follow a first-order kinetic with rate constants of  $0.5\text{ h}^{-1}$  and  $0.03\text{ h}^{-1}$  for  $S_N2$  reaction and  
296 dehydrobromination, respectively. These values were selected according to the relative contribution  
297 of 93% (sequential  $S_N2$  reaction) and 7% (dehydrobromination) observed in the experimental study  
298 of Kuntze et al. [24]. The evolution of concentration, carbon and bromine isotopic signals is  
299 simultaneously simulated for EDB, the intermediate and the end products. As shown in Fig. 6a, the  
300 two competing degradation reactions cause a decrease of the EDB concentration (blue solid line).  
301 The intermediate, bromoethylene glycol (red dotted line), is formed and further degrades into  
302 ethylene glycol (green dash-dotted line) by nucleophilic substitution ( $S_N2$ ). In parallel,  
303 dehydrobromination causes the formation of vinyl bromide (black solid line). Fig. 6b illustrates the  
304  $\delta^{13}\text{C}$  trends for the species involved in the two reaction pathways: the parent compound shows a  
305 linear behaviour, whereas the intermediate and the end products show nonlinear curves with  
306 decreasing slope. Bromine stable isotope ratios are shown in Fig. 6c. Stable bromine isotope

307 fractionation occurs at different extents for the two brominated degradation products:  $\delta^{81}\text{Br}$  is  
308 enriched by 7.6‰ for bromoethylene glycol ( $\text{S}_{\text{N}}2$  reaction) and by 1‰ for vinyl bromide  
309 (dehydrobromination), because the former is an intermediate which undergoes further  
310 debromination, whereas vinyl bromide represents a final product in this scenario. In the dual-  
311 isotope plot (Fig. 6d) a linear trend is obtained for the parent compound EDB (slope: 21.2), as well  
312 as for vinyl bromide from the dehydrobromination reaction (slope: 20.3). A nonlinear dual-isotope  
313 trend is obtained for the  $\text{S}_{\text{N}}2$  reaction intermediate, bromoethylene glycol, with a slope varying from  
314 11.1 to 22.9. The dual isotope trend of EDB (blue line in Fig. 6d) appears very similar with the one  
315 obtained during 100%  $\text{S}_{\text{N}}2$  reaction (lower dashed line). This is due to the fact that, in the  
316 considered scenario, the  $\text{S}_{\text{N}}2$  reaction is the dominant pathway (about 93% contribution) during  
317 EDB degradation in alkaline solution. The shaded grey area between the dotted lines indicates the  
318 possible range for the investigated scenario: from 100% contribution of dehydrobromination (upper  
319 bound) to 100% contribution of the  $\text{S}_{\text{N}}2$  reaction (lower bound). The dual element isotope  
320 signatures of the reaction products from the different pathways have a distinct behaviour and are  
321 different from the trend of the parent compound. The simulation results indicate that in practice it  
322 might be difficult to accurately quantify the contribution of each concurrent reaction pathway  
323 exclusively based on the observed EDB carbon and bromine isotope data. However, these  
324 simulations also demonstrate that CSIA of reaction intermediates and end products can bring new  
325 possibilities to elucidate the underlying reaction steps and to accurately quantify the contributions  
326 of individual reaction pathways.

327 **[insert Figure 6 here]**

#### 328 **4. Conclusion**

329 Dual carbon-bromine isotope investigation significantly improves the understanding of various  
330 reaction mechanisms of brominated organic compounds. Recent studies have focused on the  
331 development of analytical techniques for bromine CSIA as well as experimental investigation of  
332 degradation mechanisms of different brominated organic pollutants. In this study, we have proposed  
333 an integrated modelling approach allowing the simultaneous prediction of concentrations and dual-  
334 element isotope ratios. Our investigation focused on carbon and bromine isotope fractionation  
335 during 1,2-dibromoethane (EDB, ethylene dibromide) transformation through different reaction  
336 pathways. The proposed modelling approach tracks dual-element isotopologues. The method  
337 allowed us reproducing the carbon and bromine isotopic signal observed in experimental studies of  
338 different chemical and biotic EDB reaction pathways. The approach is based on bond-specific  
339 reaction rates and can be readily extended to cases in which different contaminants and/or reaction  
340 pathways will require tracking also isotopomers (i.e., molecules with the same number of each  
341 isotopic atom but differing in their position). Furthermore, we exemplified the model capabilities  
342 with two scenarios involving complex reaction systems with sequential and parallel reactions,  
343 respectively. In the considered case of multistep nucleophilic substitution ( $S_N2$ ) reaction,  
344 concentration and isotopic ratios of the parent compound, the intermediate and the end product were  
345 predicted based on the validated model. Different carbon and bromine isotopic behaviours of the  
346 parent compound and intermediate were obtained. In the scenario modelling of EDB degradation  
347 via two concurrent reactions, our simulation results showed that stable isotope analysis of the  
348 reaction products is beneficial, since it allows quantifying further degradation of the intermediate  
349 product in multistep reactions, as well as providing a more accurate evaluation of the individual  
350 contributions of different concurrent pathways to the overall reaction. This is particularly beneficial  
351 when one of the reaction pathways is dominant and, therefore the sole analysis of the dual isotope  
352 trend of the parent compound would not be conclusive in identifying which degradation reactions

353 are responsible for the contaminant degradation. The proposed model was applied to the specific  
354 case of EDB degradation, however it provides a framework that can be extended to other  
355 brominated compounds that may undergo degradation through different reaction pathways. The  
356 first-principle based formulation of the approach will also facilitate future model-based applications  
357 in complex environmental systems, in which both transformation and mass transfer processes may  
358 affect the observed isotope signals.

### 359 **Acknowledgements**

360 The authors thank Dr. Kevin Kuntze for providing the experimental data that were used to test the  
361 modelling approach and two anonymous reviewers for their comments that helped improving the  
362 manuscript.

363 B.J. and M.R. acknowledge the support of the Deutsche Forschungsgemeinschaft (grant RO4169/2-  
364 1) and of the Sino-Danish Center (SDC).

365 B.J. acknowledges the support of CAS Pioneer Hundred Talents Program

366

367 I.N. acknowledges the support of the Deutsche Forschungsgemeinschaft (grant FOR1530  
368 NI1329/1-2)

369

370

371

372

373

374

375

376

377

378

379

380

381 **Table 1.** Reaction mechanisms, bulk enrichment factors ( $\epsilon_{\text{bulk}}$ ) and fractionation factors at reactive position  
 382 ( $\alpha_{\text{rp}}$ ) for the different EDB degradation reactions.

Reaction	Mechanism	$\epsilon_{\text{bulk}}$		$\alpha_{\text{rp}}$	
		C	Br	C	Br
Zn (0)	dibromoelimination	-10.9±1.1	-2.1±0.3	0.9891±0.0011	0.9979±0.0003
<i>S. multivorans</i>	dibromoelimination	-5.3±0.5	-2.3±0.2	0.9947±0.0005	0.9977±0.0002
Alkaline solution	abiotic S <sub>N</sub> 2	-29.2±2.6	-1.0±0.1	0.9416±0.0052	0.9980±0.0002
<i>A. aquaticus</i>	biotic S <sub>N</sub> 2	-6.9±0.4	-0.6±0.1	0.9862±0.0008	0.9988±0.0002

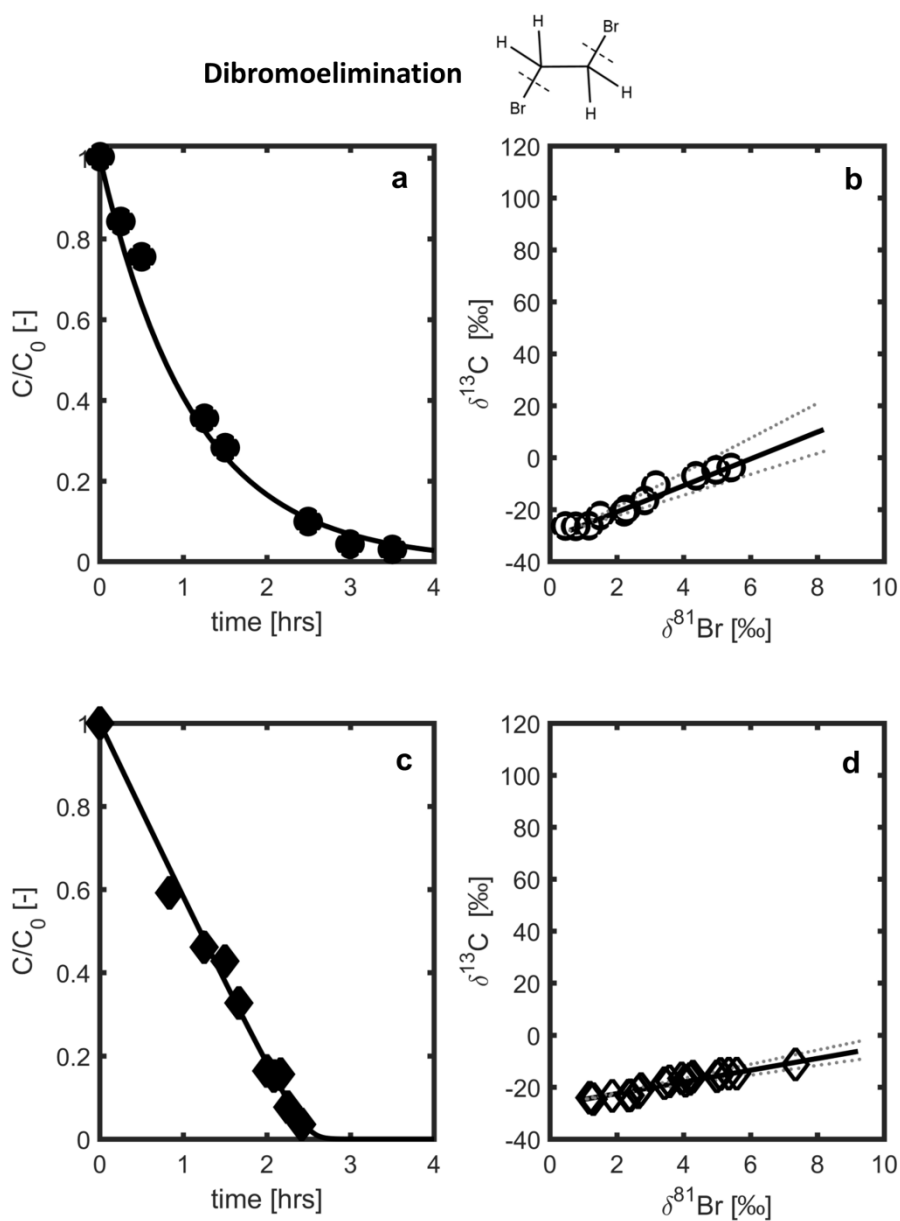
383

384

385

386

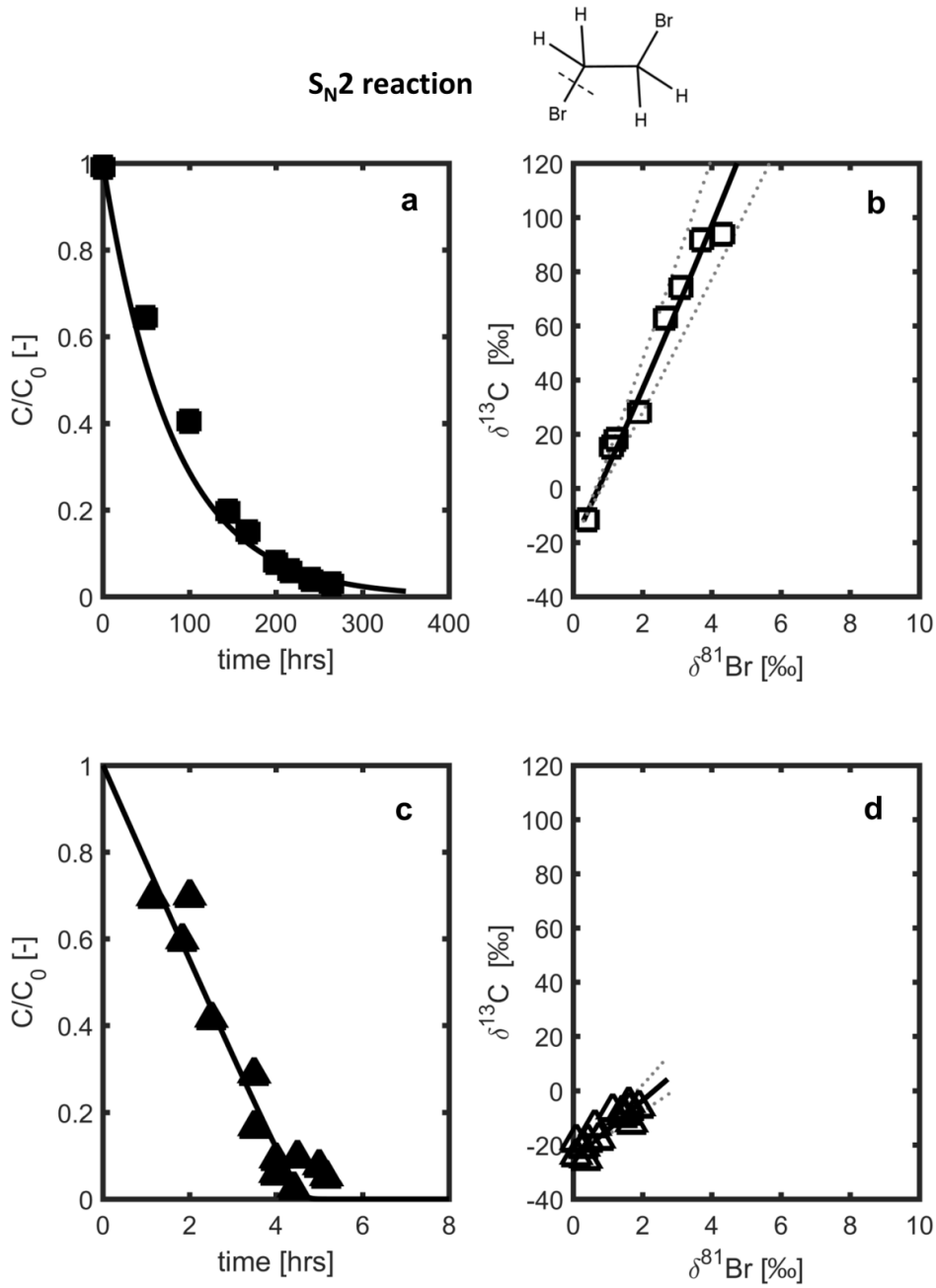
387



388

389 **Figure 1.** Concentration change and dual carbon-bromine isotope fractionation during dibromoelimination  
 390 reaction by Zn(0) (Panels (a) and (b)) and biotic reaction with *S. multivorans* (Panels (c) and (d)). The  
 391 symbols represent the experimental data reported in Kuntze et al. [24], and the solid lines are the simulation  
 392 results.

393



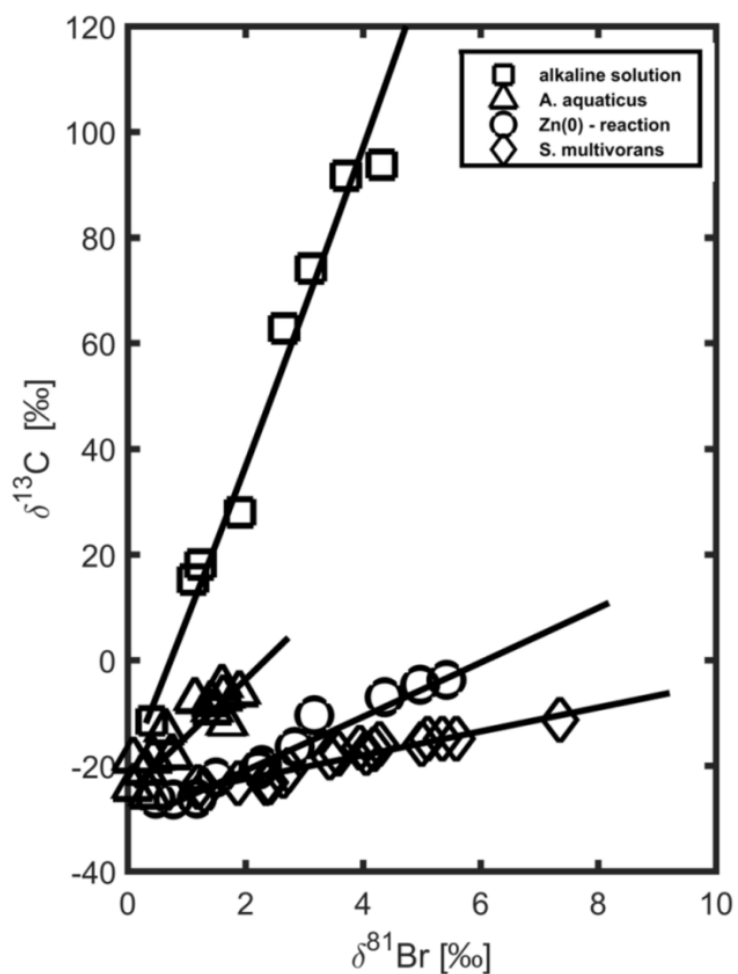
394

395 **Figure 2.** Carbon and bromine isotope fractionation during EDB chemical transformation in alkaline  
 396 solution and biotic reaction by *Ancylobacter aquaticus*. Panel (a) and (c): the symbols represent the observed  
 397 concentration profiles reported in Kuntze et al. [24], and the lines are the simulation results. Panel (b) and  
 398 (d): the symbols are carbon-bromine isotopic data and the solid lines are the simulation results.

399

400

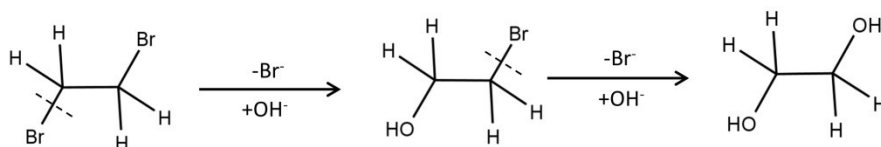
401  
402



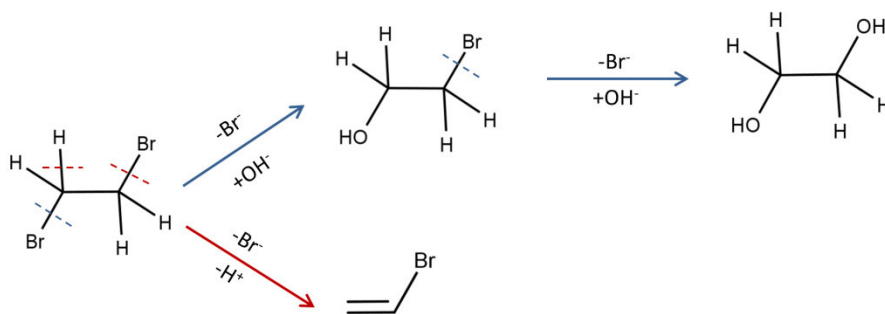
403  
404 **Figure 3.** Carbon and bromine isotope fractionation for different EDB degradation reactions. The symbols  
405 represent the experimental data reported in Kuntze et al.[24], and the solid lines represent the results of the  
406 simulations corresponding to 99% degradation of the initial EDB concentration.

407  
408  
409  
410

**Scenario 1: Multistep reactions by nucleophilic substitution (S<sub>N</sub>2)**



**Scenario 2: Parallel reactions in alkaline solution (nucleophilic substitution and dehydrobromination)**



411

412 **Figure 4.** Schemes representing the sequential and parallel reaction pathways considered in the scenario  
413 modelling.

414

415

416

417

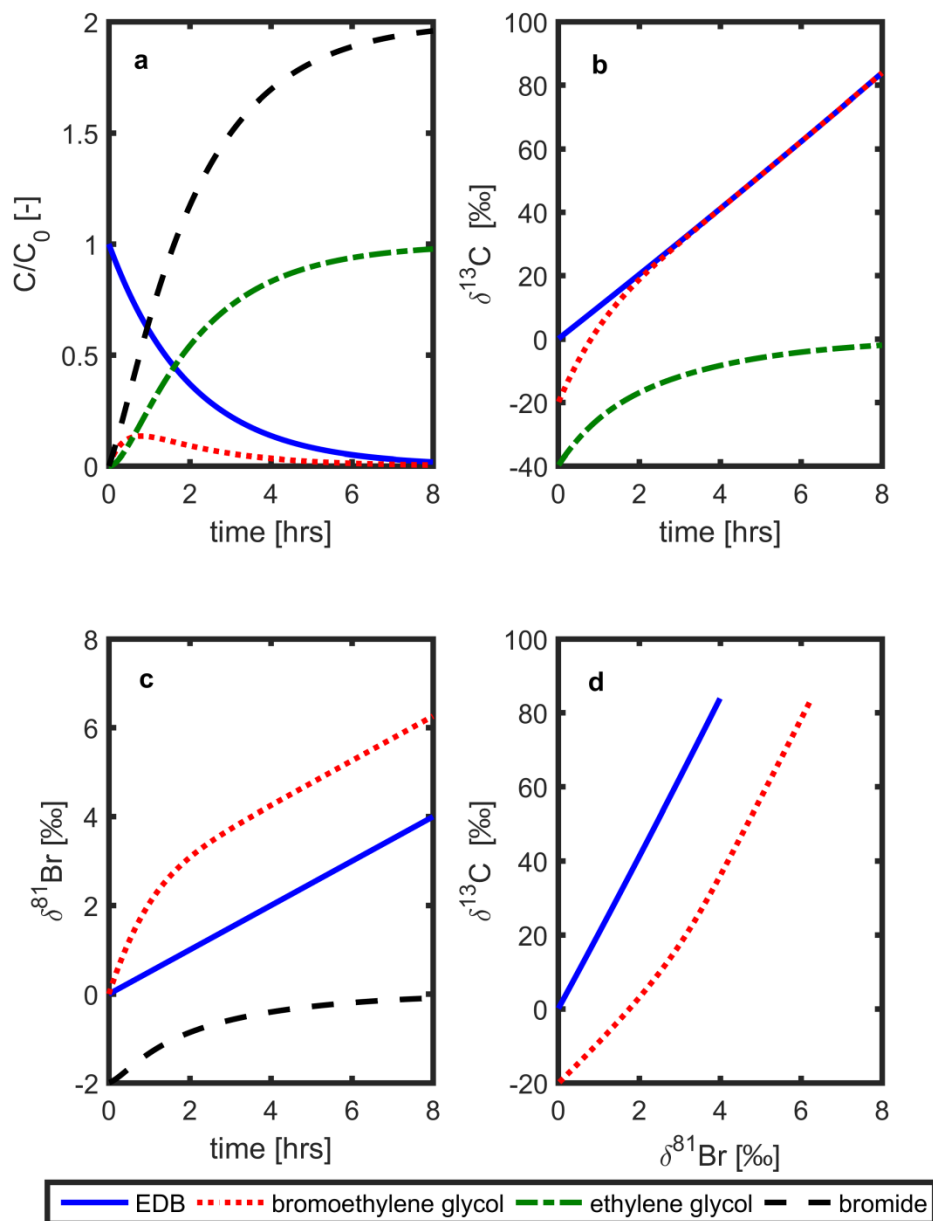
418

419

420

421

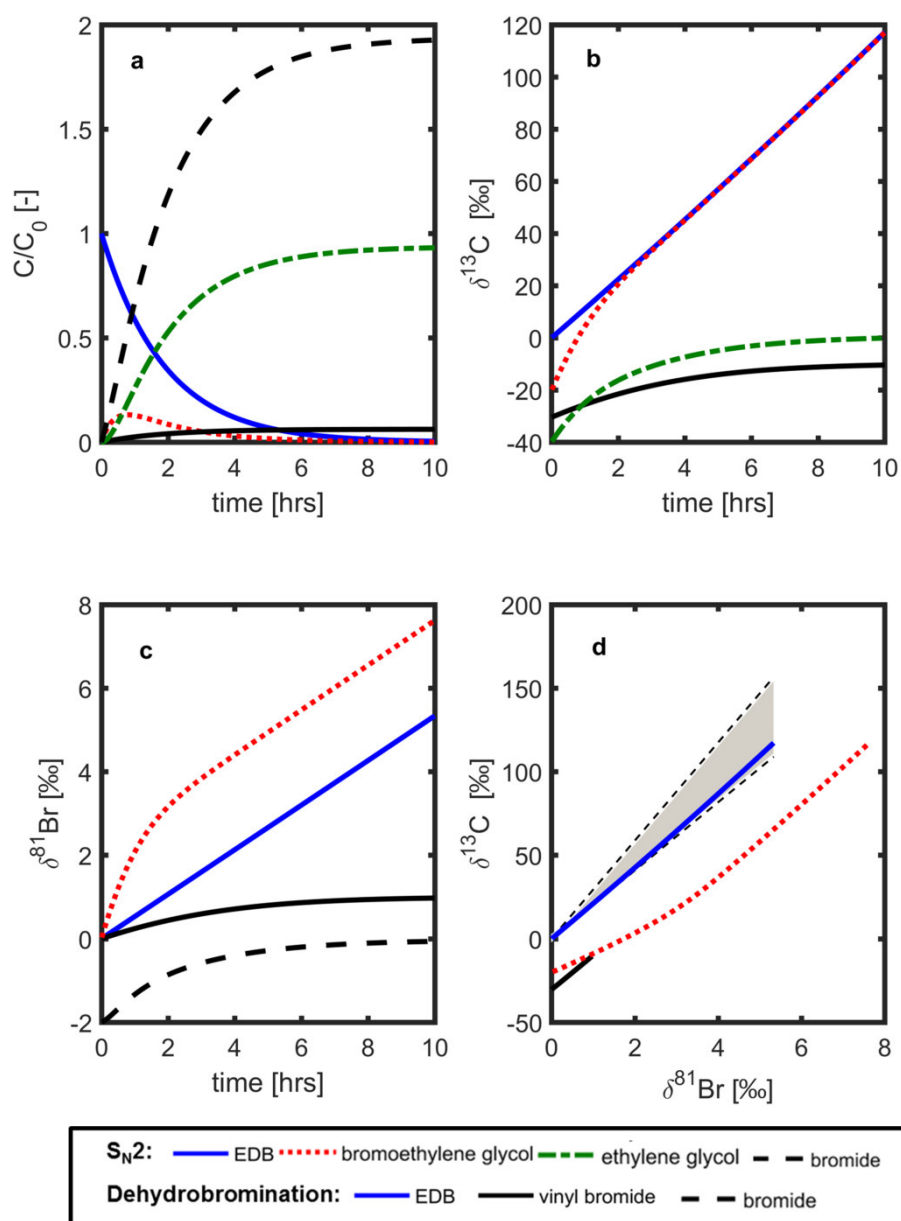
422



423

424 **Figure 5.** Concentration, carbon and bromine isotope fractionation of EDB, the intermediate (bromoethylene  
 425 glycol), the end product (ethylene glycol) and bromide during multi-step nucleophilic substitution (Scenario  
 426 1 in Fig. 4).

427



428

429 **Figure 6.** Concentration, carbon and bromine isotope fractionation of EDB during the two competing  
 430 reaction pathways: nucleophilic substitution ( $S_N2$ ) reaction and dehydrobromination (Scenario 2 in Fig. 4).

431 The shaded area in Panel (d) indicates EDB dual-isotope trends corresponding to different contributions of  
 432 each reaction pathway considered in Scenario 2. The dotted lines on the upper and lower bounds represent  
 433 dual-isotope trends of EDB degradation when one reaction pathway occurs exclusively (i.e., 100%  
 434 dehydrobromination and 100%  $S_N2$  reaction, respectively).

435

436 **References**

- 437 [1] Falta RW, Bulsara N, Henderson JK, et al. Leaded-gasoline additives still contaminate groundwater.  
438 *Environ. Sci. Technol.* 2005;39:379A–384A.
- 439 [2] Wilson, John T, Banks, Kenneth, Earle, Robert, He, Yongtian, Kuder, Tomasz, Adair C. Natural  
440 attenuation of the lead scavengers 1,2-dibromoethane (EDB) and 1,2-dichloroethane (1,2-DCA) at  
441 motor fuel release sites and implications for risk management. U.S. EPA. 2008.
- 442 [3] Yu R, Peethambaram HS, Falta RW, et al. Kinetics of 1,2-dichloroethane and 1,2-dibromoethane  
443 biodegradation in anaerobic enrichment cultures. *Appl. Environ. Microbiol.* 2013;79:1359–1367.
- 444 [4] McKeever R, Sheppard D, Nüsslein K, et al. Biodegradation of ethylene dibromide (1,2-  
445 dibromoethane [EDB]) in microcosms simulating in situ and biostimulated conditions. *J. Hazard.*  
446 *Mater.* 2012;209–210:92–98.
- 447 [5] Kuder T, Wilson JT, Philp P, et al. Carbon isotope fractionation in reactions of 1,2-dibromoethane  
448 with FeS and hydrogen sulfide. *Environ. Sci. Technol.* 2012;46:7495–7502.
- 449 [6] Bosma TNP, Middeldorp PJM, Schraa G., Zehender AJB. Mass Transfer Limitation of  
450 Biotransformation: Quantifying Bioavailability. *Environ. Sci. Technol.* 1997;31:248–252.
- 451 [7] Rolle M, Kitanidis PK. Effects of compound-specific dilution on transient transport and solute  
452 breakthrough: A pore-scale analysis. *Adv. Water Resour.* 2014;71:186–199.
- 453 [8] Schüth C, Taubald H, Bolaño N, et al. Carbon and hydrogen isotope effects during sorption of  
454 organic contaminants on carbonaceous materials. *J. Contam. Hydrol.* 2003;64:269–281.
- 455 [9] Nijenhuis I, Richnow HH. Stable isotope fractionation concepts for characterizing biotransformation  
456 of organohalides. *Curr. Opin. Biotechnol.* 2016;41:108–113.
- 457 [10] Elsner M, Imfeld G. Compound-specific isotope analysis (CSIA) of micropollutants in the  
458 environment - current developments and future challenges. *Curr. Opin. Biotechnol.* 2016;41:60–72.
- 459 [11] Schmidt TC, Jochmann M a. Origin and Fate of Organic Compounds in Water: Characterization by  
460 Compound-Specific Stable Isotope Analysis. *Annu. Rev. Anal. Chem.* 2012;5:133–155.
- 461 [12] Rosell M, Gonzalez-Olmos R, Rohwerder T, et al. Critical evaluation of the 2D-CSIA scheme for  
462 distinguishing fuel oxygenate degradation reaction mechanisms. *Environ. Sci. Technol.*  
463 2012;46:4757–4766.
- 464 [13] Sakaguchi-Söder K, Jager J, Grund H, et al. Monitoring and evaluation of dechlorination processes  
465 using compound-specific chlorine isotope analysis. *Rapid Commun. Mass Spectrom.* 2007;21:3077–  
466 3084.
- 467 [14] Jin B, Laskov C, Rolle M, et al. Chlorine Isotope Analysis of Organic Contaminants Using GC–qMS:  
468 Method Optimization and Comparison of Different Evaluation Schemes. *Environ. Sci. Technol.*  
469 2011;45:5279–5286.
- 470 [15] Gelman F, Halicz L. High precision determination of bromine isotope ratio by GC-MC-ICPMS. *Int.*  
471 *J. Mass Spectrom.* 2010;289:167–169.
- 472 [16] Hitzfeld KL, Gehre M, Richnow HH. A novel online approach to the determination of isotopic ratios  
473 for organically bound chlorine, bromine and sulphur. *Rapid Commun. Mass Spectrom.*  
474 2011;25:3114–3122.

- 475 [17] Bernstein A, Shouakar-Stash O, Ebert K, et al. Compound-Specific Chlorine Isotope Analysis: A  
476 Comparison of Gas Chromatography/Isotope Ratio Mass Spectrometry and Gas  
477 Chromatography/Quadrupole Mass Spectrometry Methods in an Interlaboratory Study. *Anal. Chem.*  
478 2011;83:7624–7634.
- 479 [18] Audí-Miró C, Cretnik S, Torrentó C, et al. C, Cl and H compound-specific isotope analysis to assess  
480 natural versus Fe(0) barrier-induced degradation of chlorinated ethenes at a contaminated site. *J.*  
481 *Hazard. Mater.* 2015;299:747–754.
- 482 [19] Nijenhuis I, Kuntze K. Anaerobic microbial dehalogenation of organohalides-state of the art and  
483 remediation strategies. *Curr. Opin. Biotechnol.* 2016;38:33–38.
- 484 [20] Cretnik S, Thoreson K a., Bernstein A, et al. Reductive dechlorination of TCE by chemical model  
485 systems in comparison to dehalogenating bacteria: Insights from dual element isotope analysis  
486 ( $^{13}\text{C}/^{12}\text{C}$ ,  $^{37}\text{Cl}/^{35}\text{Cl}$ ). *Environ. Sci. Technol.* 2013;47:6855–6863.
- 487 [21] Bernstein A, Ronen Z, Levin E, et al. Kinetic bromine isotope effect: Example from the microbial  
488 debromination of brominated phenols. *Anal. Bioanal. Chem.* 2013;405:2923–2929.
- 489 [22] Schmidt M, Lege S, Nijenhuis I. Comparison of 1,2-dichloroethane, dichloroethene and vinyl  
490 chloride carbon stable isotope fractionation during dechlorination by two *Dehalococcoides* strains.  
491 *Water Res.* 2014;52:146–154.
- 492 [23] Palau J, Cretnik S, Shouakar-Stash O, et al. C and Cl Isotope Fractionation of 1,2-Dichloroethane  
493 Displays Unique  $\delta^{13}\text{C}/\delta^{37}\text{Cl}$  Patterns for Pathway Identification and Reveals Surprising C–Cl  
494 Bond Involvement in Microbial Oxidation. *Environ. Sci. Technol.* 2014;48:9430–9437.
- 495 [24] Kuntze K, Kozell A, Richnow HH, et al. Dual Carbon–Bromine Stable Isotope Analysis Allows  
496 Distinguishing Transformation Pathways of Ethylene Dibromide. *Environ. Sci. Technol.*  
497 2016;50:9855–9863.
- 498 [25] Eckert D, Rolle M, Cirpka O a. Numerical simulation of isotope fractionation in steady-state  
499 bioreactive transport controlled by transverse mixing. *J. Contam. Hydrol.* 2012;140–141:95–106.
- 500 [26] Jin B, Rolle M, Li T, et al. Diffusive fractionation of BTEX and chlorinated ethenes in aqueous  
501 solution: Quantification of spatial isotope gradients. *Environ. Sci. Technol.* 2014;48:6141–6150.
- 502 [27] Van Breukelen BM, Rolle M. Transverse hydrodynamic dispersion effects on isotope signals in  
503 groundwater chlorinated solvents plumes. *Environ. Sci. Technol.* 2012;46:7700–7708.
- 504 [28] Hofstetter TB, Reddy CM, Heraty LJ, et al. Carbon and chlorine isotope effects during abiotic  
505 reductive dechlorination of polychlorinated ethanes. *Environ. Sci. Technol.* 2007;41:4662–4668.
- 506 [29] Hunkeler D, Van Breukelen BM, Elsner M. Modeling chlorine isotope trends during sequential  
507 transformation of chlorinated ethenes. *Environ. Sci. Technol.* 2009;43:6750–6756.
- 508 [30] Jin B, Haderlein SB, Rolle M. Integrated carbon and chlorine isotope modeling: Applications to  
509 chlorinated aliphatic hydrocarbons dechlorination. *Environ. Sci. Technol.* 2013;47:1443–1451.
- 510 [31] Kuder T, Van Breukelen BM, Vanderford M, et al. 3D-CSIA: Carbon, chlorine, and hydrogen isotope  
511 fractionation in transformation of TCE to ethene by a *dehalococcoides* culture. *Environ. Sci. Technol.*  
512 2013;47:9668–9677.
- 513 [32] Thullner M, Centler F, Richnow H-H, et al. Quantification of organic pollutant degradation in  
514 contaminated aquifers using compound specific stable isotope analysis – Review of recent  
515 developments. *Org. Geochem.* 2012;42:1440–1460.

- 516 [33] Jin B, Rolle M. Mechanistic approach to multi-element isotope modeling of organic contaminant  
517 degradation. *Chemosphere*. 2014;95:131–139.
- 518 [34] Jin B, Rolle M. Position-specific isotope modeling of organic micropollutants transformation through  
519 different reaction pathways. *Environ. Pollut.* 2016;210:94–103.
- 520 [35] Jin B, Rolle M. Joint interpretation of enantiomer and stable isotope fractionation for chiral pesticides  
521 degradation. *Water Res.* 2016;105:178–186.
- 522 [36] Elsner M, Zwank L, Hunkeler D, et al. A new concept linking observable stable isotope fractionation  
523 to transformation pathways of organic pollutants. *Environ. Sci. Technol.* 2005;39:6896–6916.
- 524
- 525